

# VIBRATION INDUCED EXCITATION OF INSTABILITY WAVES IN A BLASIUS FLOW

Erwin R. Gowree<sup>1</sup> & Christopher J. Atkin<sup>2</sup>

<sup>1</sup>Department of Aerodynamics, Energetics and Propulsion, ISAE-SUPAERO, Université de Toulouse, France

<sup>2</sup>Department of Engineering, University of East Anglia, UK

## Abstract

Here we have demonstrated that small amplitude localised vibration can artificially excite both 2D and 3D instability modes. The 2D modes were typical of Tollmien-Schlichting (TS) waves provided that the frequency of excitation lies within the unstable region of the neutral stability region obtained from linear stability theory. Further analysis of the streamwise and spanwise evolution of the instability modes identified from the temporal Fourier transform confirmed the presence of 3D oblique modes excited due to the nature of the mode shape deflection of the vibrating panel which was not uniform in the transverse direction. The effect of spanwise non-uniformity could be increased by activating the motors along the transverse direction. However, despite the higher initial forcing of the 2D TS mode from a combination of both streamwise and spanwise aligned motors, strong interaction with the 3D oblique mode led to a reduction in the growth rate of the TS wave in the farfield region.

**Keywords:** Vibration, Tollmien-Schlichting and oblique waves)

## 1. Introduction

The maturity of the natural laminar flow (NLF) and/or hybrid laminar flow control (HLFC) technologies is now encouraging us to start thinking about the in-service issues which could potentially cause the premature loss of laminarity. Much effort has been devoted toward understanding the effect of surface imperfections mainly, roughness, steps, gaps and waviness. However, during operation the aerodynamic surfaces are also subjected to vibration due to the operation of the engine and other aeroelastic or vibro-acoustic sources. Here, we look at the effect of a vibrating surface on the stability of a laminar boundary layer developing over a flat plate and the expected unstable modes are of the 2D Tollmien-Schlichting kind which exists on both 2D and 3D aerodynamic configurations.

From the "roadmap" of transition presented by Saric et al. [1] which was inspired by previous study of Morkovin et al. [2], the receptivity process was identified at the "heart" of the transition process. During the receptivity process environmental disturbances in the freestream which exist in the forms vortical and acoustic perturbations penetrate the boundary layer and excite instability waves while interacting with surface non-uniformities and inhomogeneities and also leading edge curvature. Once excited through the receptivity process instability waves grow accordingly with linear stability theory in very low turbulence environment. The effect on surface non-uniformities and leading edge have been intensively reviewed by Saric et al. [1] with an assessment of the progress made both experimentally and numerically, but the effect of vibration was only limited to leading edge oscillations. From a detailed study of Ruban et al. [3], some light was shed into the physical mechanism through which TS waves are excited from surface vibration. They postulated that a Stokes layer is generated due to pressure perturbation outside the boundary layer, the Stokes layer is unable to produce any TS wave on its own as the characteristic wavelength of the perturbation field is significantly larger than that of a TS wave. The main mechanism for the wavelength conversion is through interaction with localised wall roughness over a certain streamwise region. Through a closer coupling between the fluid and the structure, while solving the full compressible Navier-Stokes equations Visbal and Gordiner [4]

showed that even without external forcing, the aeroelastic instability caused the panel to oscillate and this triggered TS waves.

In the early 1980's, the problem of surface or wall vibration gained some interest in Novosibirsk and theoretical studies by Terent'ev [5] demonstrated that harmonic oscillations of a plate could potentially excite instability waves in the form of TS waves which grow accordingly with linear stability theory. Further experimental evidence was provided by Gilev [6] who also showed that transition due to TS instability could be delayed by damping the artificially forced TS wave by a phase-shifted excitation of the vibrating surface. This behaviour was also observed during the experiment of Kim et al. [7] but the similarity of this control technique with the Kramer-type compliant surfaces inspired by dolphin skin, in reference [8], [9] and [10] is yet to be determined. Carpenter and co-workers [11], [12], [13], [14] and [15] drew a more conclusive picture of the evolution of instability modes on compliant surfaces where it was demonstrated that the spatial extent played an important role too in the amplification or decay of the TS wave. Davies and Carpenter suggested that shorter extent of the compliant surfaces, as low as the wavelength of the TS wave was more efficient in damping the growth. To summarise, the TS mode can be manipulated by both temporal and spatial variation of the compliant or vibrating surfaces.

However in the presence of a 3D forcing in both a Poiseuille and a Blasius flow Elofsson and Alfredsson [16] and [17] respectively demonstrated that the TS mode can co-exist with the 3D oblique mode, where both can interact during the secondary growth stage and transition. In the previous studies summarised above the focus was on TS type 2D instability waves and thus the current study was aimed at assessing the effect of a vibrating surface with a 3D mode shape deflection on the excitation of instability waves in a Blasius boundary layer. The vibration rig constituted of a thin panel which was excited with miniature motors aligned along both the streamwise centre plane and the transverse plane to accentuate the spanwise forcing. The modes excited were first identified through temporal Fourier transform and their chordwise and spanwise evolution in the farfield were further analysed.

## 2. Experiment

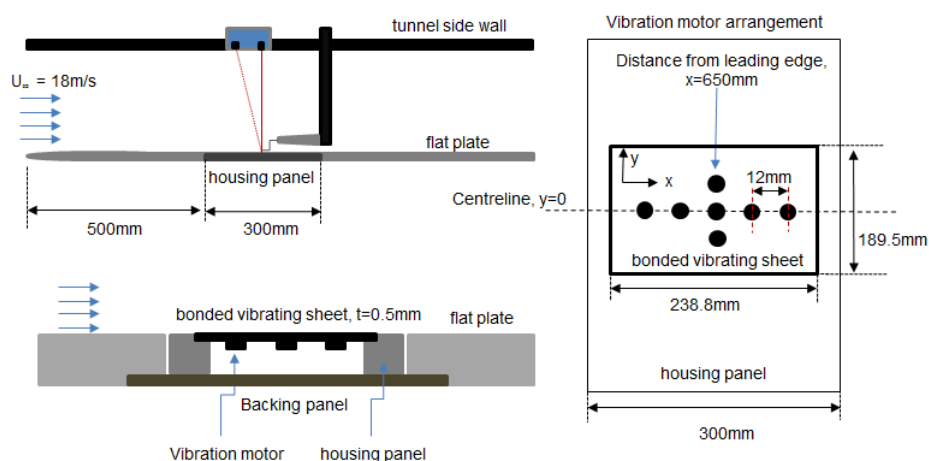


Figure 1 – Schematic illustration of the top view (right) and side view (left) of the experimental model and the vibration rig set-up

The experiment was conducted in the low turbulence wind tunnel at the Gaster Laboratory. The tunnel has a return circuit with a test section of  $0.91m \times 0.91m \times 4m$ , where a turbulence intensity level,  $Tu$ , less than 0.01% can be achieved with a flat plate model inside, for a freestream velocity ranging from  $2m/s$  to  $20m/s$  and frequency bandpass set within the range of  $2Hz$  to  $2kHz$ . Hot wire measurements were made along a  $0.91m \times 2.0m$  aluminium flat plate mounted vertically between the ceiling and the floor of the tunnel. The leading edge of the flat plate was a high aspect ratio half ellipse and also equipped with a trailing edge flap and a trim tab to adjust the location of the stagnation point and to ensure a close to zero pressure gradient condition over the majority of the plate. This was confirmed by 13 local static pressure measurements using surface mounted pressure taps. The flat plate had

a rectangular cut through starting at  $0.5m$  from the leading edge and extending to  $0.8m$ , to house the vibration rig shown schematically in figure 1. A  $0.5mm$  deep recess was machined out of the  $300mm \times 450mm$  insert panel to house a  $240mm \times 190mm \times 0.5mm$  flexible Aluminium sheet which was excited by  $12mm$  diameter Precision Microdrives coin style vibration motors mounted underneath the sheet. The vibration motors were driven by a sinusoidal voltage signal generated from NI Labview and amplified by an audio amplifier to provide the required amount of current. A series of different configurations were tested, where the motors were aligned along a single axis either along the longitudinal or the transverse axis or a combination of both. The motors were driven at the frequencies selected from the neutral stability analysis conducted by [18], where a non-dimensional frequency,  $F = 50 \times 10^{-6}$  was identified as the most amplified in the region where the excitation was applied and the amplitude of the vibration was controlled by varying the number of live motors after having chosen a desired input voltage to the motors (see reference [19]).

The motors were operating in such a way that the axis of spin was normal to the flat face which was bonded under the Aluminium sheet and therefore the primary oscillation was tangential to the wall. Due to the rigidly supported ends this also produced a normal deflection of the Al-sheet in the normal direction but significantly smaller than if the axis of spin was parallel to the surface. This was beneficial in ensuring that the deflection was of the order of microns and hence would not introduce significant amplification of the instability wave purely due to surface deformation. The mean,  $U$ , and fluctuating velocity,  $u'$ , components over the vibrating sheet was captured using hot wire anemometry, where the probe could be positioned at a desired wall reference position determined by the Micro-Epsilon laser displacement sensor which had a resolution of  $\pm 7\mu m$  and a frequency response of  $1kHz$ . A National Instruments PXI system was used for simultaneous data acquisition of the hot wire signal, pressure and temperature and control of a three axis traverse, excitation of the vibration motors and the wind tunnel speed which was obtained from a differential pressure transducer connected to a Pitot-static tube. The experiment was conducted at a freestream Reynolds number of  $1.2 \times 10^6/m$  and the hot wire signal was bandpass filtered at  $10Hz - 4kHz$  through a Krohnkite filter.

### 3. Evolution of instability modes

#### 3.1 Streamwise

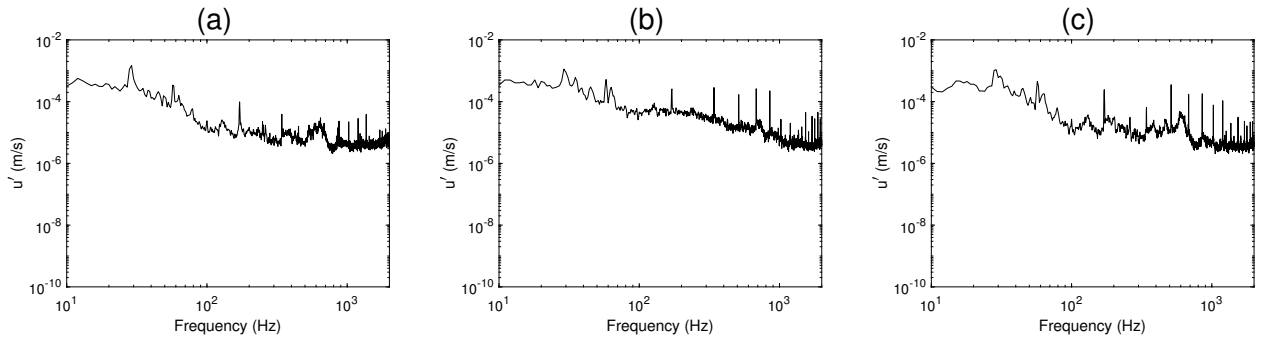


Figure 2 – Temporal Fourier transform of the hot wire signal at  $x = 650mm$  for the forcing with 1 motor in (a), 5 motors all aligned along the streamwise direction in (b) and 7 motors with five aligned along the streamwise direction and an additional two along the span and adjacent to the one in the centre in (c).

The non-dimensional frequency,  $F = 50 \times 10^{-6}$  identified by Xu et al. [18], was equivalent to  $172Hz$  and in our previous parametric analysis [19] we demonstrated that when driven at this frequency just a single motor was sufficient to excite instability waves in the form of TS waves. From a more detailed analysis in the vicinity of the forcing source, figure 2 shows that even when the amplitude of the forcing remains relatively low with only one motor active the nearfield transient is dominated by sharp harmonics of the forcing frequency. The effect of increasing the number of active motors from 1 to 7 led to an increase in the amplitude of the fundamental and the harmonics. However, for all three cases a non-negligible amount of energy is observed within the narrow frequency band of  $520$  and  $720Hz$  centred at around  $600Hz$ . The effect of frequency of forcing can be assessed while comparing

the configuration of 5 motors aligned along the symmetry plane in figure 2(b) with figure 3(a). The behaviour in the vicinity of the forcing source shows a similar picture as earlier, here it is interesting to note that the fundamental at 86Hz was slightly less energetic than the harmonics. This confirms that if the fundamental excitation frequency is not within the unstable bounds of the neutral stability curve the mode is damped. Further evidence can be seen when comparing the evolution of the unstable modes downstream in figure 3(b) and (c), where only the 172Hz appears to grow further. At  $x = 900mm$  all the near-field transients are mostly attenuated and the dominant 172Hz mode carried on growing. This was more pronounced for the 172Hz forcing as opposed to the 86Hz forcing since the initial amplitude of the fundamental 172Hz mode was much larger than the first harmonic of the 86Hz forcing. The peak at 29Hz and 58Hz was due to the vibration of the main flat plate itself and was present at all chordwise positions as seen in figure 3.

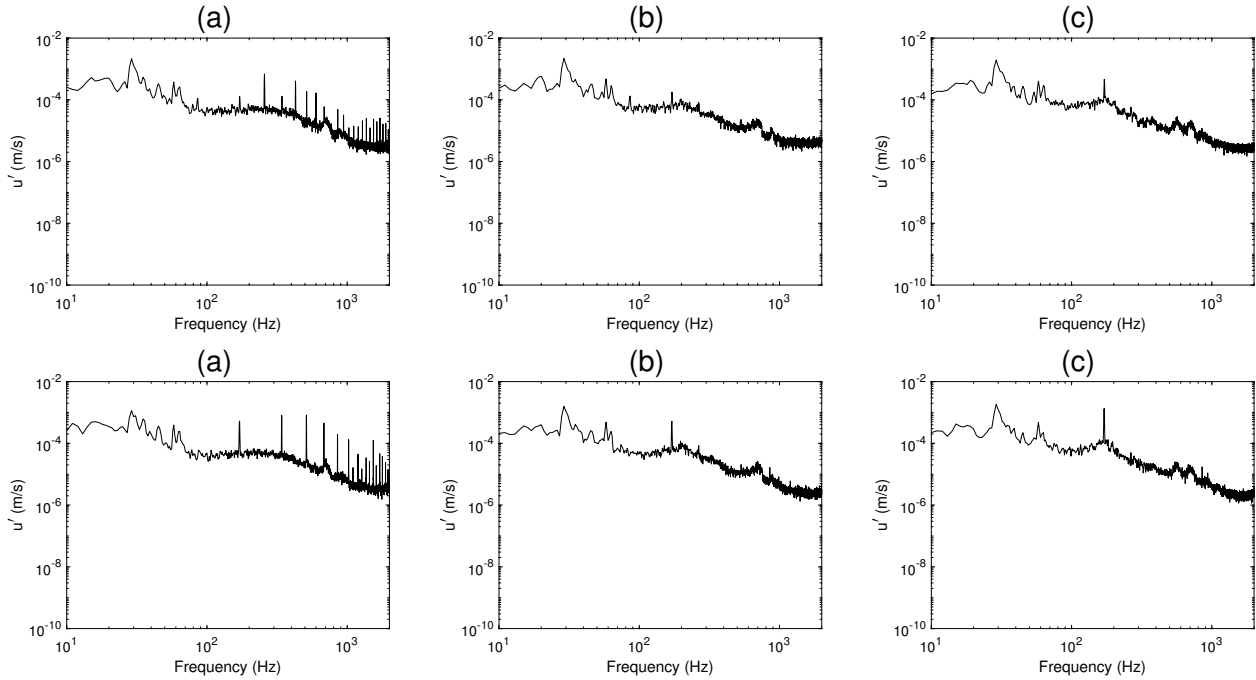


Figure 3 – Temporal Fourier transform of the hot wire signal at  $x = 700mm$ ,  $x = 900mm$  and  $1100$ , in (a), (b) and (c) respectively, for the forcing with five motors along the streamwise at 86Hz and (d), (e) and (f) at 172Hz.

The wall normal profiles of the streamwise velocity component,  $u'$ , of the first harmonic of the 86Hz and fundamental of the 172Hz forcing at  $x = 1200mm$  in figure 4(b) and (c) is representative of a 2D mode due to the presence of the dual lobe in the eigenfunction typical of a TS wave. However the large scatter in the fundamental mode from the 86Hz forcing suggests that this mode was not sufficiently developed or amplified. The TS characteristic of the 172Hz forcing can be confirmed from the phase angle profile in figure 4(f) due to the  $180^\circ$  phase angle shift about half way through the boundary layer. This phase angle shift is also present in the case of the fundamental of the 86Hz forcing mode despite a larger scatter in figure 4(d), however for the case of the first harmonic this angle was much lower, ranging from  $45^\circ$  in the near wall region to  $90^\circ$  further away in the boundary layer. Further information on the development of the excited modes can be seen in figure 5 which shows the evolution of the local maximum in  $u'$  for the first harmonic of the 86Hz and the fundamental of the 172Hz. A strong initial response is observed over the vibrating panel and the non-monotonic growth is coherent with the mode shape deflection of the panel. Both modes decayed towards the trailing edge of the excitation panel and started to recover at  $x > 750mm$  where they started growing at a similar rate but with different amplitude due to lower initial perturbation in the case of the 86Hz forcing. The exponential growth of the fundamental 172Hz mode in figure 5, together with the TS type amplitude and phase profile confirms that after recovery from the near-field this mode would grow accordingly with 2D linear stability theory. However, despite showing similar exponential growth rate and amplitude profile with the 172Hz forcing, the difference in the phase profile of the first harmonic

## Vibration Induced Excitation of Instability Waves in a Blasius Flow

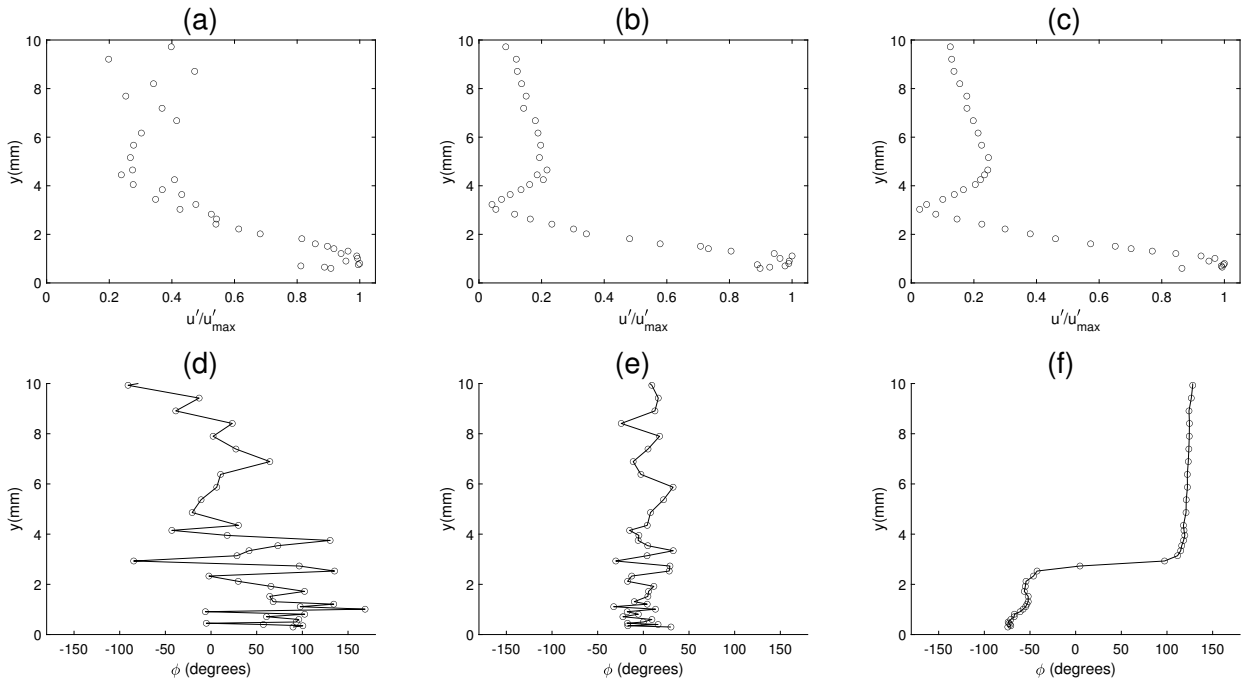


Figure 4 – The amplitude profile of the streamwise fluctuating velocity component  $u'$  of the fundamental 86Hz mode in (a), in (b) the first harmonic of the 86Hz mode and in (c) the fundamental of 172Hz mode at  $x = 1200mm$ .

of the 86Hz mode suggest interactions with other modes as seen earlier from the spectra in figure 3. This effect was more pronounced in the case of 86Hz forcing since the initial perturbation was much lower and allowed the co-existence of other modes while the sufficient forcing in the case of the 172Hz forcing where the 2D mode would dominate other 3 modes present due to the 3D nature of the mode shape deflection of the vibrating panel.

In order to intensify the 3D effects, a combination of motors aligned along the transverse plane at  $x = 650mm$  (centre of the vibrating panel) were tested as well. The excitation was fixed at 172Hz and the response of the boundary layer due to the motors aligned purely in the transverse and combination of both transverse and streamwise activated motors can be deduced from the spectra in figure 6(a) to (f) and (g) to (h) respectively, together with the evolution of these modes downstream. The effect in the near-field was similar to that reported earlier, marked by the presence of superharmonics, but here the energy content of the narrow frequency centred at around 600Hz was higher and including the subharmonics of this mode which were more pronounced even in the near-field for all the three

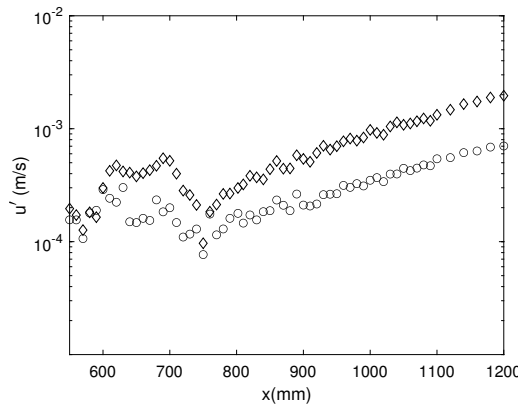


Figure 5 – The max amplitude of the streamwise fluctuating velocity component  $u'$  of the first harmonic of the 86Hz mode, '○', and the fundamental of 172Hz mode '◇' along the symmetry plane of the plate.

## Vibration Induced Excitation of Instability Waves in a Blasius Flow

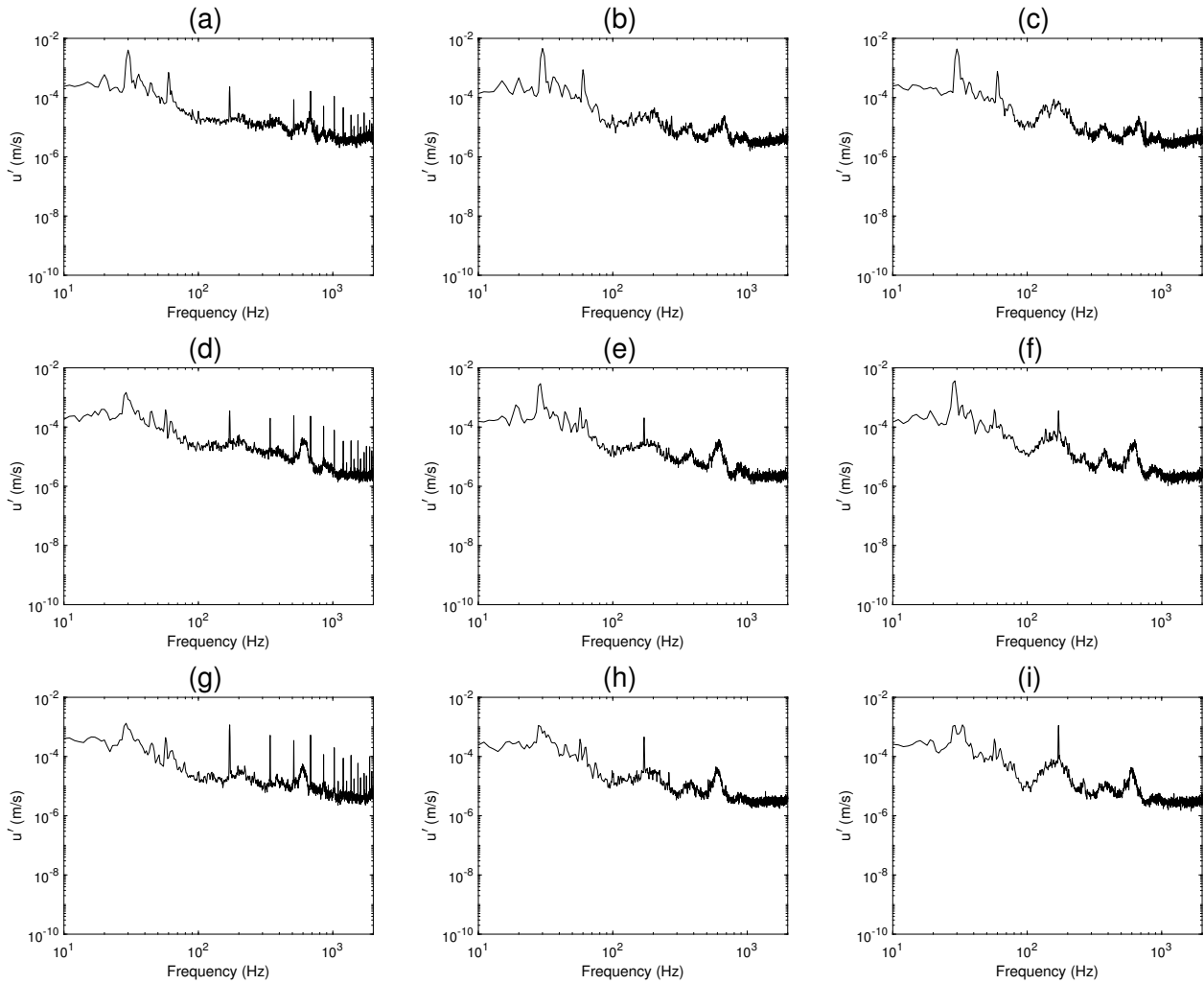


Figure 6 – Temporal Fourier transform of the hot wire signal at  $x = 700mm$ ,  $x = 900mm$  and  $1100$ , for the forcing frequency of  $172Hz$  with 3 and 5 motors along the transverse direction in (a) to (c) and (d) to (f) respectively. (g) to (i) represents the case with 5 motors along the streamwise direction and 3 along the transverse direction.

configurations tested. For the case of 3 live motors aligned along the transverse direction further downstream at  $x = 700mm$  and  $900mm$ , in figure 6(b) and (c) respectively the  $172Hz$  mode was masked out within the narrow frequency band of  $100$  to  $220Hz$  which corresponds to the subharmonic of the mode centred at around  $600Hz$ . In the case of 5 live motors along the transverse direction in figure 6(e) and (f), and five motors in the streamwise and 3 motors along the transverse direction (7 motors in total) in figure 6(h) and (i) the  $172Hz$  mode was still present unlike in the case of the 3 live transverse motors. Once again this was due to the higher initial forcing provided by larger number of active motors in these configurations. But for the same number of active motors, in the case of 5 along the transverse plane, the mode centred around  $600Hz$  and the subharmonics were more pronounced in figure 6 (f) compared with the case of 5 active motors aligned along the streamwise direction in figure 3 (f) at the same farfield streamwise position.

The presence of dual lobes in the amplitude profile and the  $180^\circ$  shift in the phase angle profile shown in figure 7(b) and (e) for the case of 5 motors along the transverse direction and figure 7(c) and (f) for 5 streamwise and 3 transverse motors confirms that at  $x = 1100mm$ , the  $172Hz$  mode was typical of a TS mode. For the 3 transverse motors the scatter in the amplitude profile was larger and the phase angle shift of approximately  $45^\circ$  would point to the fact that this was not a pure 2D mode. The growth rate of the  $172Hz$  mode from these transverse forcing configurations can be compared with the case of 5 live motors aligned purely along the streamwise direction in figure 8. Despite achieving similar levels of amplitude and trend in the nearfield the two cases with 5 motors show significant difference

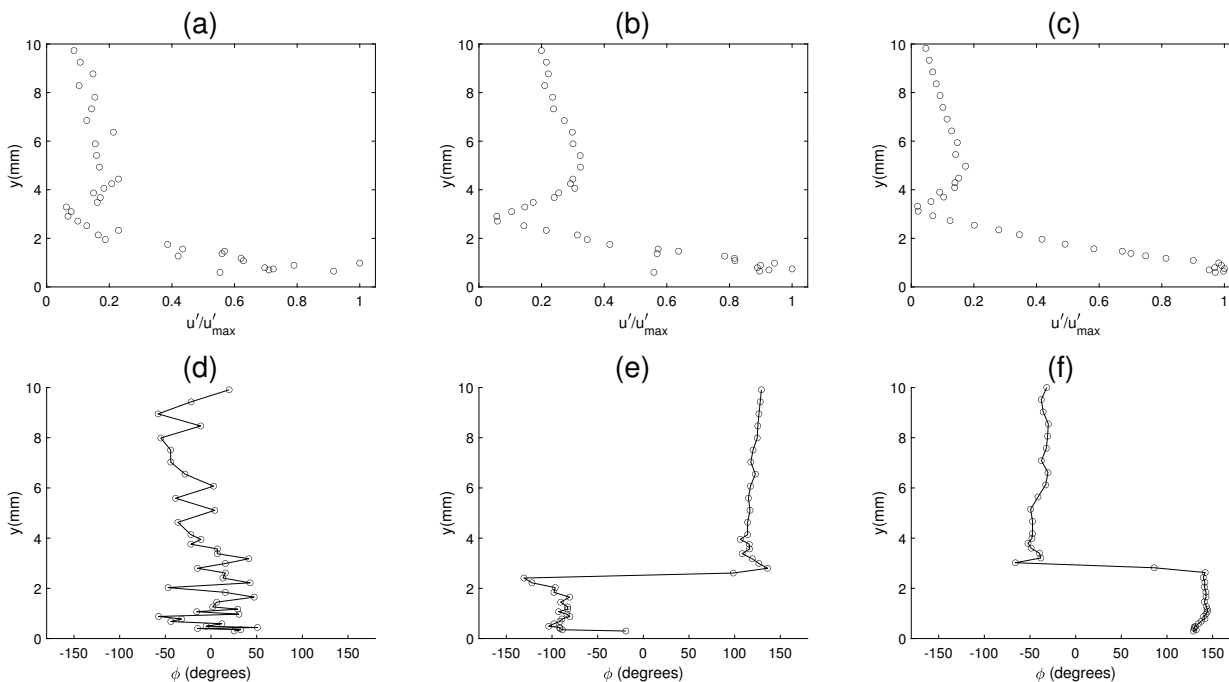


Figure 7 – The amplitude profile of the streamwise fluctuating velocity component  $u'$  and phase angle profile of the 172Hz excitation at  $x = 1100\text{mm}$  with 3 and 5 live motors aligned in the transverse direction in (a) and (d), and (b) and (e) respectively and for the case of 5 motors along the streamwise direction and 3 in the transverse direction in (e) and (f).

in the growth rate after the recovery region at  $x > 750\text{mm}$ . The case with 5 motors along the transverse direction grew at a much lower rate than that of 5 motors along the streamwise direction which grew exponentially. Referring back to figure 4(c) and (f) and figure 7(b) and (e) in both cases with 5 motors the amplitude and the phase profiles exhibited TS like behaviour, however the difference in the growth rate after the recovery would suggest that there might be an interaction with other modes. In fact the in the case of 5 transverse motor the mode started to saturate at  $x > 1100\text{mm}$ , since the harmonics of the 172Hz mode were damped as seen in figure 2(e) and (f), the saturation was not related to non-linear interactions. While comparing the case with 5 motors in streamwise and 3 in transverse against that with 5 motors only along the streamwise direction the nearfield amplitude from the total of 7 motors are higher but they recover downstream and starts growing at similar levels at  $x > 750\text{mm}$ . But regardless of the higher initial forcing the growth rate with the sum of 7 motors was slightly lower thereafter and started to saturate at  $x > 1000\text{mm}$  while reaching similar amplitude to that with 5 motors along the transverse direction. Since here as well the higher harmonics of the 172Hz were damped the saturation in amplitude could not be attributed to non-linearity and would therefore point towards interaction with oblique modes which are intensified by the three dimensionalisation accentuated by the transversely aligned motors.

When excited with 3 transverse motors the amplitude of the near field is much lower and the recovery region is prolonged further downstream to  $x > 950\text{mm}$  and at this point the growth rate is similar to that of 5 motors along the transverse axis but a lower overall amplitude. Earlier, from figure 6 the 172Hz mode which corresponds to the 2D mode appeared to decay downstream and this was further confirmed 7(a) and (d). The growth here is therefore due to the bump in the spectra within the frequency band of of 100 to 220Hz which correspond to the subharmonic of the band centred around 600Hz present in all cases. From earlier studies of Elofsson and Alfredsson [16] and [17] oblique transition was demonstrated to be through interaction of subharmonic modes, therefore this encouraged further investigation into the spanwise development of the instabilities.

### 3.2 Spanwise evolution

The spanwise evolution of the unstable modes identified above is further analysed here. From the local maximum amplitude in the streamwise velocity fluctuation,  $u'$ , along the spanwise plane at

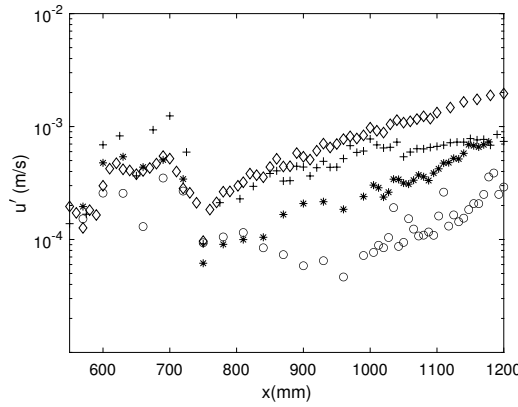


Figure 8 – The max amplitude of the streamwise fluctuating velocity component  $u'$ , for the forcing frequency of 172Hz with 5 motors aligned in the symmetry plane ‘ $\diamond$ ’ and an additional two transverse motors (7 motors total) ‘+’. ‘ $\circ$ ’ represents a 3 motors and ‘\*’, 5 motors all aligned in the transverse direction long the centre of the vibrating panel.

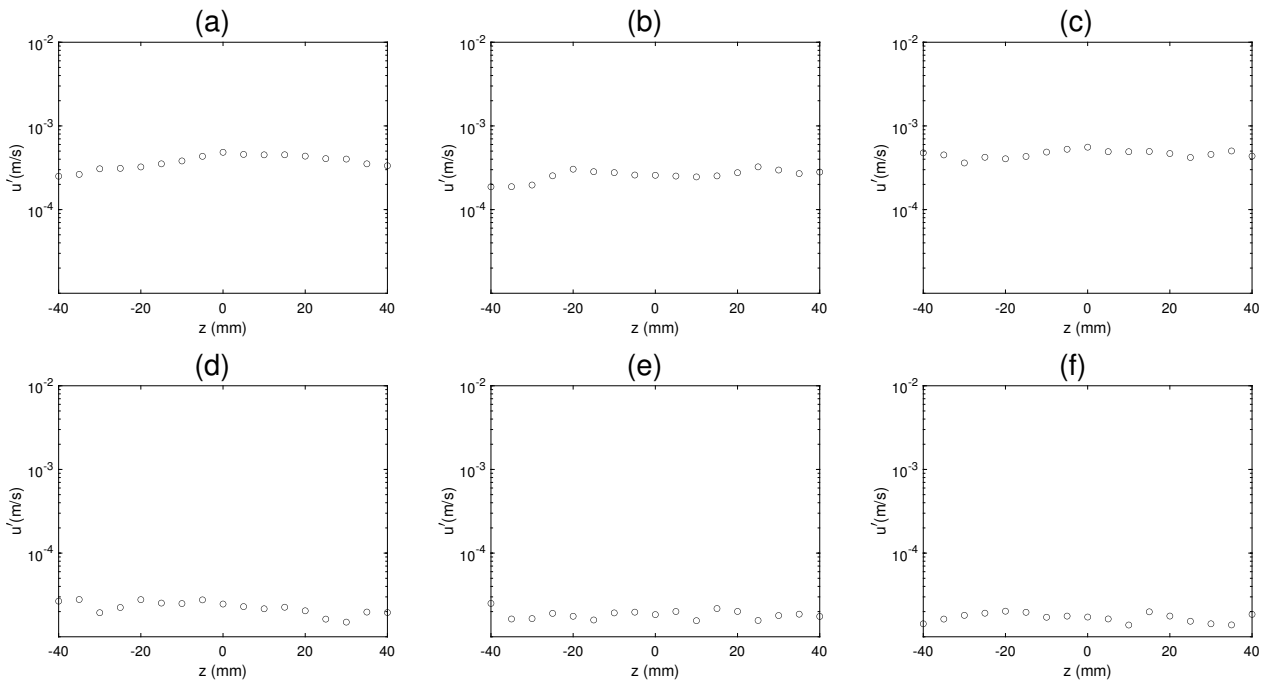


Figure 9 – The maximum amplitude the streamwise fluctuating velocity component  $u'$  of the fundamental 172Hz mode top and the 600Hz mode bottom at  $x = 700mm$ ,  $x = 900mm$  and  $x = 1100mm$  in (a) and (d), (b) and (e), and (c) and (f) respectively, forced by 5 motors along the streamwise.

$x = 700$  in figure 9(a) even when forced with motors aligned purely along the streamwise direction the 172Hz mode was seen to be distorted in the spanwise direction too, within the nearfield region of the forcing itself. This effect is clearer for the case of two additional transverse motors in figure 10(a) due to the larger amplitude forcing. During the earlier analysis, further downstream this mode showed TS like behaviour based on the fluctuating velocity and phase amplitude profile and the growth rate. But in figure 9 (b) and (c) the same mode developed a wave-like feature in the local maximum amplitude in the spanwise plane at both  $x = 900mm$  and  $x = 1100mm$  this would suggest that this mode was interacting with a 3D mode. The theoretical analysis of Craik [20] showed that a TS wave and a pair of oblique wave can interact and undergo very rapid non-linear growth. But here the maximum amplitude attained was significantly lower than 1% of the freestream velocity which normally indicates the beginning of non-linearity and from figure 8 the case with 3 and 5 transverse motors started growing again at  $x = 1000mm$  after the recovery from the near-field. In the case of the mode centred at around 600Hz the wave-like behaviour in the spanwise distribution



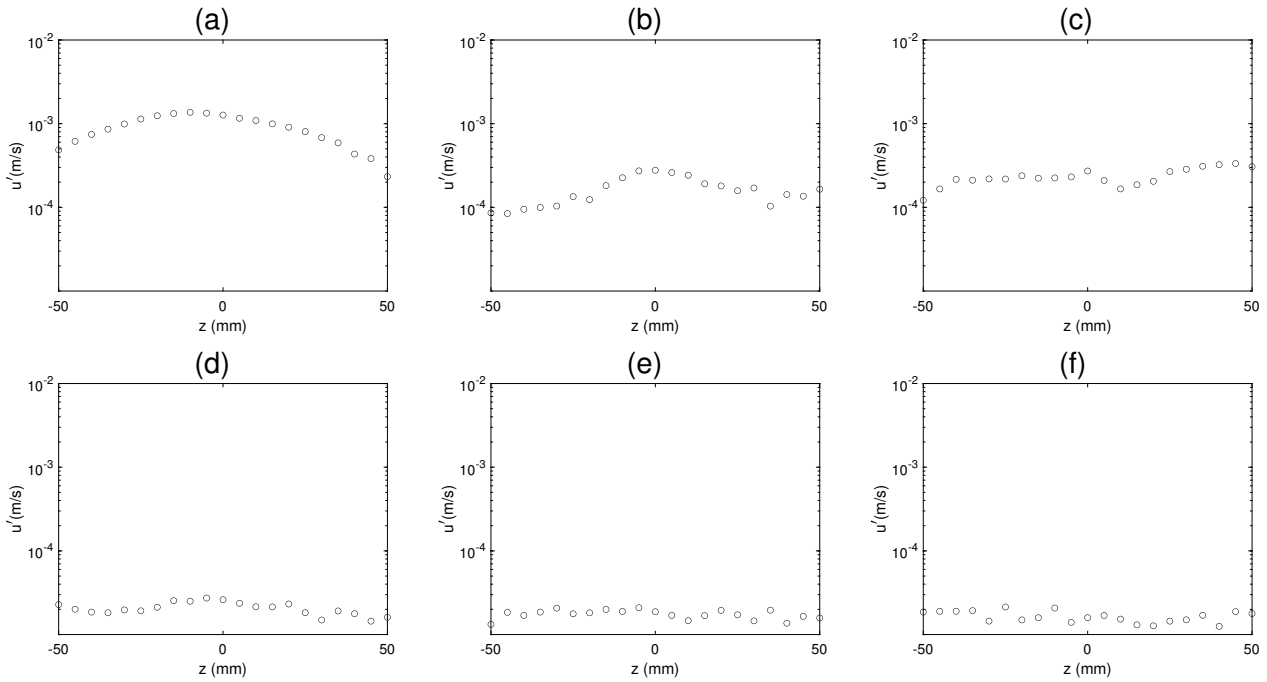


Figure 10 – The maximum amplitude the streamwise fluctuating velocity component  $u'$  of the fundamental 172Hz mode top and the 600Hz mode bottom at  $x = 700mm$ ,  $x = 900mm$  and  $x = 1100mm$  in (a) and (d), (b) and (e), and (c) and (f) respectively, forced by 5 motors along the streamwise and 3 along the transverse direction

in maximum  $u'$  was present right from the nearfield region in both the case with 5 motors purely in the streamwise direction and that with additional two motors, in figure 9(d) and 10(d) respectively. This effect was more pronounced further downstream where the average overall amplitude dropped slightly in both excitation cases. This is further evidence that the mode centred around 600Hz is an oblique mode which is promoted by the 3D nature of the mode shape deflection and intensified in the presence of transversely aligned motors, since the wave-like behaviour was accentuated in the presence of two additional transverse motors when comparing figure 9 (e) and (f) with figure 10 (e) and (f). Referring back to Elofsson and Alfredsson's work the oblique mode would still grow exponentially, in this case further analysis will be required to extract the wave-number of the mode and track it's growth downstream.

#### 4. Summary

Considerable experimental and numerical evidence have shown that surface vibration can excite Tollmien-Schlichting waves which is 2D in nature. Here, we have provided further confirmation that if the frequency of excitation lies within the unstable bounds of the neutral stability curve a TS wave can be excited even if the amplitude of the surface deflection is of the order of microns. Since the response of the boundary layer in the vicinity of the source was dominated by harmonics of the fundamental forcing frequency, even if the frequency of excitation was not an unstable mode, if any of the harmonics were within this unstable region of the neutral curve they would develop further downstream. This has not been reported previously in the literature.

Previous studies of the effect of surface vibration have focussed mainly on the excitation of TS wave without any emphasis on the effect due to non-uniformity of the excitation source along the spanwise direction. This was the main objective of the current study and the spanwise non-uniformity in the forcing was accentuated by transversely orientated motors. The analysis along the centre plane showed that all the cases with the motors along the streamwise direction were able to generate instability waves which would first recover and then develop into TS waves further downstream, however the temporal Fourier transform showed the presence of other modes whose frequency did not coincide with the frequency of forcing. Further analysis showed that these modes were fully 3D and were more pronounced when the motors aligned in the transverse direction were activated. Sufficient

evidence suggested that the 3D mode is oblique in nature especially when the forcing was applied purely in the transverse direction with only 3 active motors, which ensured that the 2D mode was very weak and did not grow significantly downstream. For the case of 5 motors along the streamwise direction when the 2D TS mode was sufficiently amplified, an additional two transverse motors led to a strong interaction between the TS mode and a subharmonic of the 3D oblique mode. This led to a reduction in the growth rate of the 2D TS mode, which was even lower than the case with 5 motors only, along the streamwise direction. Therefore, this suggests that a well controlled 3D mode can interact with a 2D TS mode in such a way the growth rate of the later can be reduced and thus delaying the transition process. Provided that the 3D mode itself does not undergo very rapid non-linear growth which would favour immediate breakdown.

## 5. Acknowledgments

The authors would like to thank Prof Michael Gaster for his recommendations during the experimental campaign and Innovate UK for their financial support to the SANTANA project under grant No. 113001

## 6. Contact Author Email Address

mailto:erwin-ricky.gowree@isae-superaero.fr

## 7. Copyright Statement

The authors confirm that they, and/or their company or organization, hold copyright on all of the original material included in this paper. The authors also confirm that they have obtained permission, from the copyright holder of any third party material included in this paper, to publish it as part of their paper. The authors confirm that they give permission, or have obtained permission from the copyright holder of this paper, for the publication and distribution of this paper as part of the ICAS proceedings or as individual off-prints from the proceedings.

## References

- [1] W. Saric, H. Reed, and E. J. Kerschen, "Boundary-layer receptivity to freestream disturbances," *Annual Review of Fluid Mechanics*, vol. 34, no. 1, pp. 291–319, 2002.
- [2] M. Morkovin, E. Reshotko, and T. Herbert, "Transition in open flow systems a reassessment," *Bulletin of American Physical Society*, vol. 39, p. 1882, 1994.
- [3] A. I. Ruban, T. Bernots, and D. Pryce, "Receptivity of the boundary layer to vibrations of the wing surface," vol. 723, p. 480, 2013.
- [4] M. Visbal and R. Gordnier, "Numerical simulation of the interaction of a transitional boundary layer with a 2-d flexible panel in the subsonic regime," *Journal of Fluids and Structures*, vol. 19, no. 7, pp. 881 – 903, 2004.
- [5] E. Terent'ev, "The linear problem of a vibrator in a subsonic boundary layer," *Journal of Applied Mathematics and Mechanics*, vol. 45, no. 6, pp. 791 – 795, 1981.
- [6] V. M. Gilev, "Tollmien-schlichting waves excitation on the vibrator and laminar-turbulent transition control," in *Laminar-Turbulent Transition* (V. V. Kozlov, ed.), p. 243, IUTAM Symposium Novosibirsk, USSR, Springer-Verlag, 1984.
- [7] S. Y. Kim, X. Bonnardel, J. P. Guibergia, and E. Brocher, "Transitional boundary-layer response to wall vibrations," *Smart Materials and Structures*, vol. 3, no. 1, p. 6, 1994.
- [8] M. O. Kramer, "Boundary layer stabilization by distributed damping," *Journal of the American Society for Naval Engineers*, vol. 72, no. 1, pp. 25–34, 1960.
- [9] M. O. Kramer, "The dolphins' secret," *Journal of the American Society for Naval Engineers*, vol. 73, no. 1, pp. 103–108, 1961.
- [10] M. T. Landahl, "On the stability of a laminar incompressible boundary layer over a flexible surface," *Journal of Fluid Mechanics*, vol. 13, no. 4, p. 609–632, 1962.
- [11] P. Carpenter, "The effect of a boundary layer of the hydroelastic instability of infinitely long plates," *Journal of Sound and Vibration*, vol. 93, no. 3, pp. 461–464, 1984.
- [12] P. W. Carpenter and A. D. Garrad, "The hydrodynamic stability of flow over kramer-type compliant surfaces. part 1. tollmien-schlichting instabilities," *Journal of Fluid Mechanics*, vol. 155, p. 465–510, 1985.
- [13] P. W. Carpenter and A. D. Garrad, "The hydrodynamic stability of flow over kramer-type compliant surfaces. part 2. flow-induced surface instabilities," *Journal of Fluid Mechanics*, vol. 170, p. 199–232, 1986.

- [14] C. Davies and P. W. Carpenter, "Numerical simulation of the evolution of tollmien–schlichting waves over finite compliant panels," *Journal of Fluid Mechanics*, vol. 335, p. 361–392, 1997.
- [15] A. Lucey, P. Sen, and P. Carpenter, "Excitation and evolution of waves on an inhomogeneous flexible wall in a mean flow," *Journal of Fluids and Structures*, vol. 18, no. 2, pp. 251 – 267, 2003. Axial and Internal Flow Fluid-Structure Interactions.
- [16] P. A. ELOFSSON and P. H. ALFREDSSON, "An experimental study of oblique transition in plane poiseuille flow," *Journal of Fluid Mechanics*, vol. 358, p. 177–202, 1998.
- [17] P. A. Elofsson and P. Alfredsson, "An experimental study of oblique transition in a blasius boundary layer flow," *European Journal of Mechanics - B/Fluids*, vol. 19, no. 5, pp. 615–636, 2000.
- [18] H. Xu, S. M. Mughal, E. R. Gowree, C. J. Atkin, and S. J. Sherwin, "Destabilisation and modification of tollmien-schlichting disturbances by a three-dimensional surface indentation," *Journal of Fluid Mechanics*, vol. 819, pp. 592–620, 2017.
- [19] E. R. Gowree and C. J. Atkin, "On the excitation of tollmien-schlichting waves due to surface vibration," International Symposium of Applied Aerodynamics, Lyon, 2017.
- [20] A. D. D. Craik, "Non-linear resonant instability in boundary layers," *Journal of Fluid Mechanics*, vol. 50, no. 2, p. 393–413, 1971.